JOURNAL OF MATERIALS SCIENCE 21 (1986) 2073–2082

The development of cavity growth maps for superplastic materials

ATUL H. CHOKSHI*
Materials Science Department, University of Southern California, Los Angeles, California 90089-0241, USA

Superplastic alloys usually deform to very large extents but excessive cavitation can lead to premature cavitation failure in these materials. Several mechanisms can contribute to the growth of cavities during superplastic deformation although, generally, there is only one mechanism that controls cavity growth. Cavity growth mechanisms of relevance to superplastic materials are analysed in detail and the possible transitions in rate-controlling cavity growth mechanisms are considered. The contribution of lattice diffusion to the diffusional growth of cavities is included in the overall analysis of cavity growth. Cavity growth maps are constructed to show the dominant cavity growth mechanisms under different experimental conditions. Equations are developed to predict the appropriate transitions in cavity growth mechanisms with increasing cavity radii. Finally, it is demonstrated that the predictions of the cavity growth maps are consistent with the experimental results in several superplastic materials.

1. Introduction

Superplastic materials generally exhibit extremely large uniform elongations prior to failure. It is now recognized that most superplastic materials cavitate during deformation [1, 2]. Excessive cavitation during deformation is detrimental to the mechanical properties of superplastic materials [3, 4] and this may limit the subsequent commercial use of superplastic alloys. Consequently, considerable research activity has been directed recently towards developing a better understanding of cavitation in superplastic materials. It is known that cavitation failure occurs by the nucleation, growth and interlinkage of cavities; among these stages, the process of cavity growth is reasonably well understood.

Cavities that form during superplastic deformation may grow by one or more of several mechanisms. A knowledge of the cavity growth rate equations enables the determination of the individual contributions of these mechanisms to the overall cavity growth rate. In general, cavity growth occurs predominantly by one of several mechanisms. The purpose of developing cavity growth maps is to display pictorially the experimental conditions over which different cavity growth mechanisms dominate the overall growth of cavities. These maps will conceivably provide considerable assistance in analysing and predicting cavity growth in superplastic materials that are tested under different experimental conditions. Such cavity growth maps are similar to the deformation mechanism maps [5–8] and the fracture maps [9] that were developed earlier.

Svennson and Dunlop [10, 11] constructed cavity growth maps for high temperature creep conditions and they showed that the predictions of these maps were consistent with the experimental observations of cavity growth. Miller and Langdon [12] developed a cavity growth map for high temperature creep; they noted specifically that the map was not applicable to the growth of cavities which intersect more than one grain boundary. In fine-grained superplastic materials cavities are observed frequently with sizes greater than the grain size.

The ability of these maps to predict the dominant cavity growth process depends critically on the use of appropriate cavity growth mechanisms in constructing the maps. Consequently, Section 2 is devoted to a comprehensive analysis of cavity growth in superplastic materials. Following this, different types of cavity growth maps are developed and the possible transitions in cavity growth mechanisms are discussed. Finally, it is demonstrated that the predictions of the cavity growth maps developed in this study are consistent with the experimental results in several superplastic materials.

2. Analysis of cavity growth mechanisms

Cavity growth mechanisms developed for high temperature creep conditions have been used successfully to study cavity growth in superplastic materials [2, 13, 14]. These cavity growth mechanisms may be classified into two broad categories: diffusional cavity growth and power-law cavity growth. For superplastic materials, the diffusional cavity growth mechanism that is most pertinent is the one developed under the assumption that surface diffusion is

* *Present address*: Division of Materials Science, Department of Mechanical Engineering, University of California, Davis, California 95616, USA.

0022–2461/86 $03.00 + .12

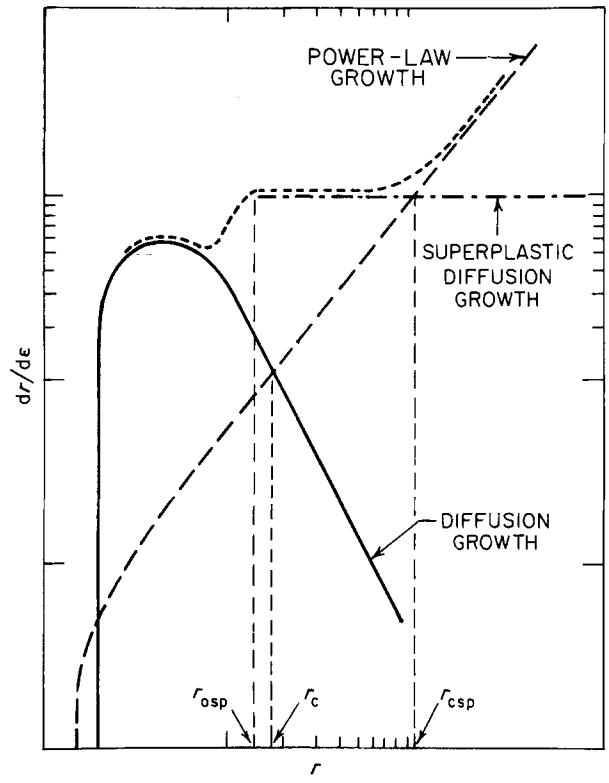

Figure 1 Schematic illustration of the variation in the cavity growth rate against the cavity radius for the diffusional, superplastic diffusional and power-law growth mechanisms.

sufficiently rapid for cavities to maintain their equilibrium shape.

The diffusional growth of cavities occurs by the stress directed diffusion of vacancies from a zone in the grain boundary plane adjacent to the cavity. The model was developed for large grained materials in which several cavities are uniformly distributed on grain boundaries that are perpendicular to the tensile axis [15]. A detailed analysis by Beere and Speight [16] indicates that the diffusional cavity growth rate is

$$\frac{dr}{d\varepsilon} = \frac{2\Omega\delta D_{gb}}{kT}\frac{1}{r^2}\left(\frac{\sigma - 2\gamma/r}{\dot{\varepsilon}}\right)\alpha \qquad (1)$$

where r is the cavity radius, ε is the true strain, $dr/d\varepsilon$ is the cavity growth rate, Ω is the atomic volume, δ is the grain boundary width, D_{gb} is the grain boundary diffusivity, k is Boltzmann's constant, T is the absolute temperature, σ is the flow stress, γ is the surface energy, $\dot{\varepsilon}$ is the strain rate and α is the cavity size-spacing parameter. The cavity size-spacing parameter is given as

$$\alpha = \frac{1}{4\ln(\lambda/2r) - [1 - (2r/\lambda)^2][3 - (2r/\lambda)^2]} \qquad (2)$$

where λ is the inter-cavity spacing. Analyses of cavity growth in superplastic materials suggest that the diffusional cavity growth mechanism is important only during the early stages of cavity growth [2, 13, 14]. During the initial stages of cavitation, the cavities are usually small and fairly well separated. Calculations indicate that, under these conditions, it is reasonable to assume a constant value of $\alpha = 0.1$ [2]. Therefore, putting $\alpha = 0.1$ in Equation 1, the diffusional cavity growth rate is

$$\frac{dr}{d\varepsilon} = \frac{\Omega\delta D_{gb}}{5kT}\frac{1}{r^2}\frac{(\sigma - 2\gamma/r)}{\dot{\varepsilon}} \qquad (3)$$

It is interesting to note that, using a different approach, Dobes and Cadek [17] developed a similar relationship for the growth of small and well-separated cavities.

Hancock [18] developed an equation for the power-law growth of cavities by modifying McClintock's [19] analysis of ductile fracture at low temperatures. The power-law growth of cavities occurs by the plastic deformation of the material surrounding a cavity. The power-law cavity growth rate is [18]

$$\frac{dr}{d\varepsilon} = r - \left(\frac{3\gamma}{2\sigma}\right) \qquad (4)$$

Inspection of fine-grained superplastic materials after deformation frequently reveals the presence of cavities with sizes greater than the grain size. Under such conditions, it is necessary to modify the diffusional cavity growth rate to account for the increase in the number of paths (grain boundaries) through which vacancies may diffuse into a cavity [13]. A new model, termed the superplastic diffusional growth model, was developed for the diffusional growth of cavities which intersect more than one grain boundary [2]. This model predicts the following cavity growth rate [2, 20]:

$$\frac{dr}{d\varepsilon} = \frac{45\Omega\delta D_{gb}}{kT}\frac{1}{d^2}\frac{\sigma}{\dot{\varepsilon}} \qquad (5)$$

where d is the grain size.

A complete analysis of cavity growth in fine-grained superplastic materials must include all of the above three mechanisms. The cavity growth rates due to these mechanisms are plotted schematically against the cavity radius in Fig. 1. In Fig. 1, r_c is cavity radius at which the diffusional growth rate is equal to the power-law growth rate and r_{csp} is the cavity radius at which the superplastic diffusional growth rate is equal to the power-law growth rate. It is to be noted that the superplastic diffusional growth model can be invoked only at r_{osp} when cavities intersect more than one grain boundary. These three cavity growth mechanisms act independently and therefore cavity growth is controlled by the mechanism that leads to the most rapid growth rate. Fig. 1 indicates that small cavities will initially grow by the diffusional growth mechanism until they intersect more than one grain boundary. At $r = r_{osp}$ there is a transition from the diffusional to the superplastic diffusional growth mechanism so that cavities with radii between r_{osp} and r_{csp} will grow by the superplastic diffusional growth mechanism. At $r = r_{csp}$ there is a transition from the superplastic diffusional to the power-law growth mechanism and cavities with radii greater than r_{csp} will grow by the power-law growth mechanism. The transitions between the different mechanisms are given by the values of r_{osp}, r_c and r_{csp}: these values will depend on the testing conditions. The variations in the transition radii with experimental conditions will be used as a basis to construct cavity growth maps in Section 3.

2.1. The significance of lattice diffusion in diffusional cavity growth

In general, the diffusional growth of cavities can occur by the diffusion of vacancies either through the lattice or along grain boundaries. In the original treatment of the diffusional growth problem, Hull and Rimmer [15] showed that grain boundary diffusion dominates lattice diffusion for their experimental conditions. The diffusional growth model was therefore developed with the assumption that vacancies diffused into cavities along grain boundaries [15, 16]. At high temperatures, typically $\gtrsim 0.8T_m$, where T_m is the absolute melting point, lattice diffusion is likely to play an increasingly important role in the diffusional growth of cavities. Burton [21] and Raj and Ashby [22] developed models that included contributions to diffusional cavity growth from both lattice diffusion and grain boundary diffusion. The relative importance of lattice and grain boundary diffusion can be gauged by determining the value of a parameter termed ψ:

$$\psi = \frac{\lambda D_l}{\pi \delta D_{gb}} \tag{6}$$

where D_l is the lattice diffusivity. The significance of Equation 6 is that when ψ is less than one, grain boundary diffusion is the dominant vacancy diffusion path whereas when ψ is greater than one, lattice diffusion is the dominant diffusion path. Following Equation 3, under conditions where lattice diffusion controls cavity growth, the diffusional cavity growth rate is:

$$\frac{dr}{d\varepsilon} = \frac{\Omega \lambda D_l}{5\pi kT} \frac{1}{r^2} \frac{(\sigma - 2\gamma/r)}{\dot{\varepsilon}} \tag{7}$$

It is important to note that the superplastic diffusional growth model cannot be invoked when lattice diffusion dominates diffusional cavity growth because that model was developed only for conditions where grain boundary diffusion controls diffusional cavity growth. Thus, when lattice diffusion is the relevant diffusion path for vacancies, cavity growth can occur by either the diffusion or the power-law growth mechanism. These two mechanisms are plotted schematically in Fig. 2 as $dr/d\varepsilon$ against r. In Fig. 2, r_c' is the cavity radius at which the lattice diffusional cavity growth rate is equal to the power-law cavity growth rate. Fig. 2 predicts that cavities with radii less than r_c' will grow by a lattice diffusional growth mechanism whereas those with radii greater than r_c' will grow by a power-law growth mechanism.

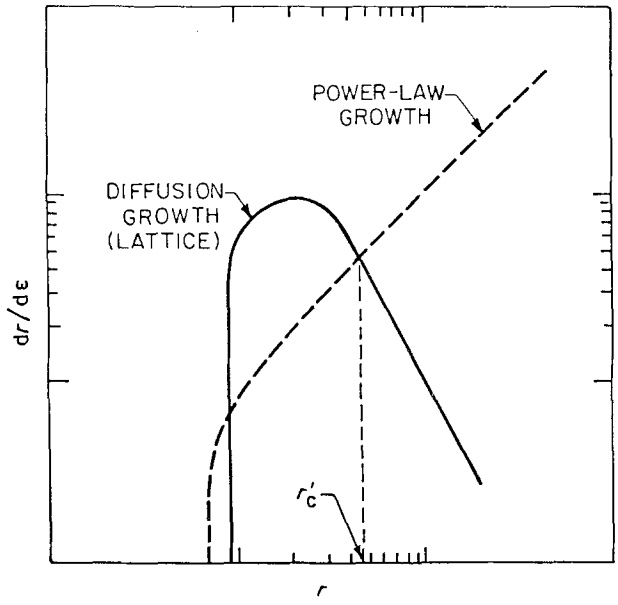

Figure 2 Schematic illustration of the variation in the cavity growth rate against the cavity radius for the lattice diffusional and the power-law growth mechanisms.

TABLE I Cavity growth mechanisms in fine-grained superplastic materials

Mechanism	Cavity Growth Rate
Diffusion (Grain boundary)	$\frac{dr}{d\varepsilon} = \frac{\Omega \delta D_{gb}}{5kT} \frac{1}{r^2} \frac{(\sigma - 2\gamma/r)}{\dot{\varepsilon}}$
Superplastic Diffusion	$\frac{dr}{d\varepsilon} = \frac{45\Omega \delta D_{gb}}{kT} \frac{1}{d^2} \frac{\sigma}{\dot{\varepsilon}}$
Power-law	$\frac{dr}{d\varepsilon} = r - \frac{3\gamma}{2\sigma}$
Diffusion (Lattice)	$\frac{dr}{d\varepsilon} = \frac{\Omega \lambda D_l}{5\pi kT} \frac{1}{r^2} \frac{(\sigma - 2\gamma/r)}{\dot{\varepsilon}}$

3. Construction of cavity growth maps

The cavity growth rate equations for the mechanisms considered in this analysis are summarized in Table I. The diffusional growth rate equation in Table I assumes that grain boundary diffusion is dominant; lattice diffusion dominant diffusion cavity growth is listed in Table I as diffusional cavity growth (lattice). These cavity growth mechanisms operate independently so that cavity growth will be controlled by the mechanism that leads to the highest value of $dr/d\varepsilon$. Cavity growth maps will be constructed for conditions where either grain boundary diffusion or lattice diffusion is the dominant vacancy diffusion path.

In order to construct the cavity growth maps it is necessary to determine the variations in the transitions between the different mechanisms as a function of the experimental parameters. It is assumed for the purpose of this analysis that the cavities are large enough that the terms $2\gamma/r$ and $3\gamma/2\sigma$ in Equations 3 and 4, respectively, can be neglected. The value of r_c, the critical radius for a transition from the diffusional to the power-law growth mechanism, is obtained by combining Equations 3 and 4:

$$r_c = \left(\frac{\Omega \delta D_{gb}}{5kT} \frac{\sigma}{\dot{\varepsilon}}\right)^{1/3} \tag{8}$$

The value of r_{csp}, the critical radius for a transition from the superplastic diffusional to the power-law growth mechanism, is obtained by combining Equations 4 and 5:

$$r_{csp} = \frac{45\Omega \delta D_{gb}}{kT} \frac{1}{d^2} \frac{\sigma}{\dot{\varepsilon}} \tag{9}$$

The superplastic diffusional growth model can be invoked only when a cavity intersects more than one grain boundary. In general, this occurs when the cavity radius is equal to half the grain size. Thus:

$$r_{osp} = d/2 \tag{10}$$

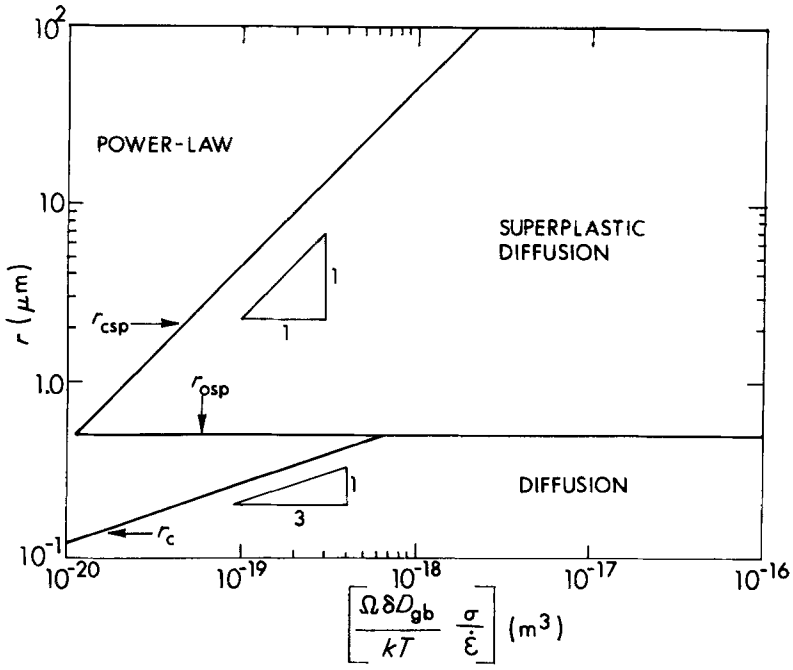

Figure 3 A cavity growth map of cavity radius against the parameter $\Omega\delta D_{gb}\sigma/kT\dot{\varepsilon}$ for a superplastic material with a grain size of 1 μm.

Equations 8 to 10 can be used to construct two types of cavity growth maps. First, cavity growth maps can be developed for a constant grain size to show the variation in cavity radius with the parameter $\Omega\delta D_{gb}\sigma/kT\dot{\varepsilon}$. Second, cavity growth maps can be constructed to depict the variation in cavity radius with grain size for a fixed value of the parameter $\Omega\delta D_{gb}\sigma/kT\dot{\varepsilon}$.

3.1. Cavity growth maps of r against $\Omega\delta D_{gb}\sigma/kT\dot{\varepsilon}$

Fig. 3 shows a cavity growth map for a superplastic material with a grain size of 1 μm and it depicts the variations in the dominant cavity growth mechanisms with cavity radii and the parameter $\Omega\delta D_{gb}\sigma/kT\dot{\varepsilon}$. Fig. 3 covers cavity radii between 0.1 and 100 μm and variations in the parameter $\Omega\delta D_{gb}\sigma/kT\dot{\varepsilon}$ between 10^{-20} and 10^{-16} m^3. The following procedure was used to construct the map:

(i) The transition between the diffusional and power-law growth mechanisms, Equation 8, was drawn such that when $r = r_c = 0.5\,\mu$m, the parameter $\Omega\delta D_{gb}\sigma/kT\dot{\varepsilon} = 6.4 \times 10^{-19}\,m^3$. The transition line has a slope of 1/3 and it is marked as r_c in Fig. 3.

(ii) The horizontal line in Fig. 3 corresponds to the cavity radius, r_{osp}, at which the cavity intersects more than one grain boundary. It follows from Equation 10 that for a material with a grain size of 1 μm, the horizontal line marked r_{osp} in Fig. 3 should be drawn at $r = r_{osp} = 0.5\,\mu$m.

(iii) The transition between the superplastic diffusional and the power-law growth mechanisms was drawn with a slope of unity. The position of the line was identified by noting that when $r = r_{csp} = 1\,\mu$m, the parameter $\Omega\delta D_{gb}\sigma/kT\dot{\varepsilon} = 2.2 \times 10^{-20}\,m^3$, Equation 9. This line is marked as r_{csp} in Fig. 3.

Fig. 4 shows a similar cavity growth map for a

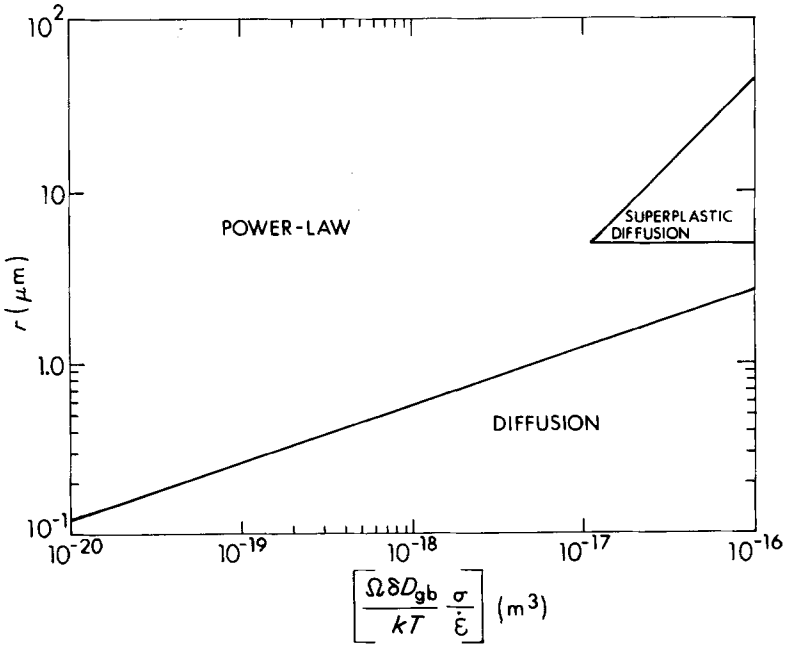

Figure 4 A cavity growth map of cavity radius against the parameter $\Omega\delta D_{gb}\sigma/kT\dot{\varepsilon}$ for a superplastic material with a grain size of 10 μm.

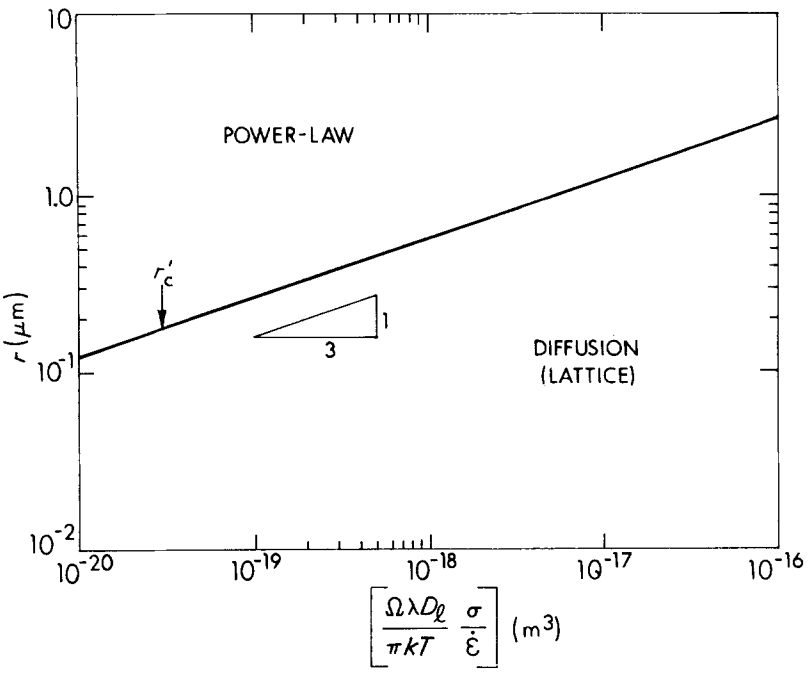

Figure 5 A cavity growth map of cavity radius against the parameter $\Omega\lambda D_l\sigma/\pi kT\dot{\varepsilon}$ for a superplastic material deformed at elevated temperatures.

superplastic material with a grain size of 10 μm. It is to be noted from a comparison of Figs 3 and 4 that an increase in the grain size significantly reduces the superplastic diffusional cavity growth field. The possible transitions in cavity growth mechanisms are discussed in detail in Section 4.

3.1.1. A map for lattice diffusional cavity growth

As noted in Section 2.1, under conditions of lattice diffusion dominance, cavity growth may occur by either the power-law growth mechanism or the lattice diffusional cavity growth mechanism. Again, neglecting the $3\gamma/2\sigma$ and the $2\gamma/r$ terms in Equations 4 and 7, respectively, the critical radius for a transition from the lattice diffusion controlled to the power-law growth mechanism, r_c', can be determined by combining Equations 4 and 7:

$$r_c' = \left[\frac{\Omega\lambda D_l}{5\pi kT}\frac{\sigma}{\dot{\varepsilon}}\right]^{1/3} \quad (11)$$

Fig. 5 shows a cavity growth map for these conditions. The transition between the lattice diffusional and power-law growth mechanisms, Equation 11, was drawn such that when $r = r_c' = 1\,\mu$m, the parameter $(\Omega\lambda D_l\sigma/\pi kT\dot{\varepsilon}) = 5 \times 10^{-18}\,\text{m}^3$. The transition line has a slope of 1/3 and it is marked as r_c' in Fig. 5.

3.2. Cavity growth maps of r against d

Fig. 6 shows a cavity growth map for a superplastic material deformed under conditions where the parameter $\Omega\delta D_{gb}\sigma/kT\dot{\varepsilon} = 10^{-18}\,\text{m}^3$. It covers cavity radii between 0.1 and 100 μm and grain sizes between 0.1 and 100 μm. The following procedure was used to construct the map:

(i) The transition between the diffusional and the power-law growth mechanisms is independent of the grain size and Equation 8 predicts that for $\Omega\delta D_{gb}\sigma/kT\dot{\varepsilon} = 10^{-18}\,\text{m}^3$, $r = r_c = 0.58\,\mu$m. Therefore, this transition is represented by a horizontal line at $r = r_c = 0.58\,\mu$m and it is marked as r_c in Fig. 6.

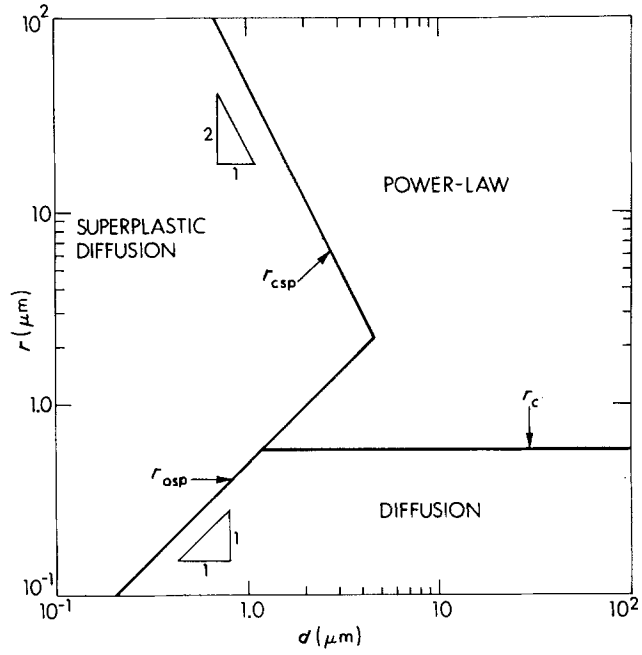

Figure 6 A cavity growth map of cavity radius against the grain size for a superplastic material that is deformed when $\Omega\delta D_{gb}\sigma/kT\dot{\varepsilon} = 10^{-18}\,\text{m}^3$.

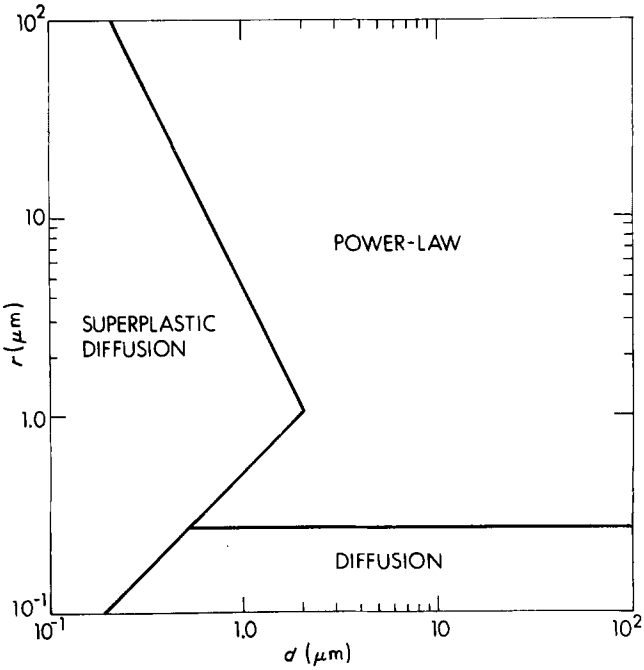

Figure 7 A cavity growth map of cavity radius against the grain size for a superplastic material that is deformed when $\Omega\delta D_{gb}\sigma/kT\dot{\varepsilon} = 10^{-19}\,m^3$.

(ii) The superplastic diffusional growth model can be invoked only at $r = r_{osp} = d/2$. Therefore, the onset of the superplastic diffusional growth mechanism is depicted by a straight line with a slope of unity and it is marked as r_{osp} in Fig. 6. From Equation 10, the position of this line was identified by noting that when $d = 1.0\,\mu m$, $r = r_{osp} = 0.5\,\mu m$.

(iii) The transition between the superplastic diffusion and the power-law growth mechanisms is given by the line marked as r_{csp} in Fig. 6. Following Equation 9, this line was drawn with a slope of -2 and it was positioned such that when $d = 1\,\mu m$, $r = r_{csp} = 45\,\mu m$.

A similar cavity growth map is shown in Fig. 7 for the value of the parameter $\Omega\delta D_{gb}\sigma/kT\dot{\varepsilon} = 10^{-19}\,m^3$. An inspection of Fig. 6 indicates that for $\Omega\delta D_{gb}\sigma/kT\dot{\varepsilon} = 10^{-18}\,m^3$, the superplastic diffusional cavity growth model is relevant only up to a maximum grain size of $4.5\,\mu m$ whereas Fig. 7 indicates that for $\Omega\delta D_{gb}\sigma/kT\dot{\varepsilon} = 10^{-19}\,m^3$, the superplastic diffusional growth model is relevant only up to maximum grain size of $\sim 2.1\,\mu m$. The above observations suggest that an increase in the value of $\sigma/\dot{\varepsilon}$, corresponding to experiments conducted at lower strain rates, leads to increase in the maximum grain size up to which the superplastic diffusional growth model is relevant.

4. Analysis and discussion

In order to avoid repetition, this section will focus largely on the cavity growth maps shown in Figs 3 and 4. The other types of cavity growth maps, Figs 5 and 7, can be analysed in a similar manner.

A close inspection of Figs 3 and 4 reveals that, depending upon the experimental condition, the growth of cavities could lead to three different series of transitions in cavity growth mechanisms. With increasing cavity radii, these series of transitions in cavity growth mechanisms are:

(a) diffusion to superplastic diffusion to power-law,

(b) diffusion to power-law to superplastic diffusion to power-law, and

(c) diffusion to power-law.

Equations will be developed now to predict the series of transitions in cavity growth mechanisms that will occur under any set of experimental conditions.

An examination of Fig. 3 indicates that the (a) series of transitions occurs when $\Omega\delta D_{gb}\sigma/kT\dot{\varepsilon} \gtrsim 6.3 \times 10^{-19}\,m^3$. In general, these transitions will occur when

$$r_c \gtrsim r_{osp} \tag{12}$$

Combining Equations 8 and 10 with Equation 12 results in the following condition for the occurrence of the (a) series of transitions:

$$\left(\frac{\Omega\delta D_{gb}}{kT}\frac{\sigma}{\dot{\varepsilon}}\right) \gtrsim \frac{5}{8}d^3 \tag{13}$$

It is to be noted that in accordance with Fig. 3, Equation 13 predicts the occurrence of the (a) series of transitions when $\Omega\delta D_{gb}\sigma/kT\dot{\varepsilon} \gtrsim 6.3 \times 10^{-19}\,m^3$ for a grain size of $1\,\mu m$.

Fig. 3 indicates that the (b) series of transitions in cavity growth mechanisms occur when $1.1 \times 10^{-20}\,m^3 \lesssim \Omega\delta D_{gb}\sigma/kT\dot{\varepsilon} \lesssim 6.3 \times 10^{-19}\,m^3$. In general, an inspection of Figs 3 and 4 reveals that the (b) series of transition will occur when

$$\left.\begin{aligned} r_c &\lesssim r_{osp} \\ \text{and} \qquad r_{csp} &\gtrsim r_{osp} \end{aligned}\right\} \tag{14}$$

The combination of the above equation with Equations 8 to 10 indicates that the (b) series of transitions will occur when

$$\frac{d^3}{90} \lesssim \frac{\Omega\delta D_{gb}}{kT}\frac{\sigma}{\dot{\varepsilon}} \lesssim \frac{5}{8}d^3 \tag{15}$$

An inspection of Fig. 4 reveals that the (c) series of transitions in cavity growth mechanism occurs when $\Omega\delta D_{gb}\sigma/kT\dot{\varepsilon} \lesssim 1.1 \times 10^{-17}\,m^3$. In general, these

TABLE II Conditions for the occurrence of different series of transitions in cavity growth mechanisms

Series of transitions	Conditions
Diffusion to superplastic diffusion to power law	$\frac{\Omega\delta D_{gb}}{kT}\frac{\sigma}{\dot{\varepsilon}} \gtrsim \frac{5}{8}d^3$
Diffusion to power-law to superplastic diffusion to power-law	$\frac{d^3}{90} \lesssim \frac{\Omega\delta D_{gb}}{kT}\frac{\sigma}{\dot{\varepsilon}} \lesssim \frac{5}{8}d^3$
Diffusion to power-law	$\frac{\Omega\delta D_{gb}}{kT}\frac{\sigma}{\dot{\varepsilon}} \lesssim \frac{d^3}{90}$

transitions will occur when

$$r_{csp} \lesssim r_{osp} \tag{16}$$

The following general condition is obtained by combining Equation 16 with Equations (9) and (10):

$$\frac{\Omega\delta D_{gb}}{kT}\frac{\sigma}{\dot{\varepsilon}} \lesssim \frac{d^3}{90} \tag{17}$$

An important consequence of the above analysis is that when Equation 17 is satisfied, it is not necessary to consider the superplastic diffusional growth model for cavity growth. This simplifies the construction of the cavity growth maps since the transition from the diffusion to the power-law growth mechanism is independent of the grain size. The conditions for the occurrence of the above three series of transitions are summarized in Table II.

Fig. 5 is a cavity growth map for conditions when lattice diffusion is the dominant vacancy diffusion path. It is not necessary to re-construct this cavity growth map for different superplastic materials since the transition from the lattice diffusional to the power-law growth mechanism is independent of the grain size.

An examination of Figs 6 and 7 indicates that, depending upon the experimental conditions, there are three possible series of transitions in cavity growth mechanisms. The conditions for the observation of these series of transitions are the same as those given by Equations 13, 15 and 17. A comparison of Figs 3 to 7 reveals that the superplastic diffusional growth model is likely to play an important role during cavity growth in superplastic materials only when the grain size is small and the specimens are deformed at low strain rates and intermediate temperatures.

It is important to note that the above cavity growth maps were developed by neglecting the $2\gamma/r$ and $3\gamma/2\sigma$ terms in the cavity growth rate equations. Therefore, these cavity growth maps cannot be used to predict the transitions in cavity growth mechanisms at relatively small cavity radii. At small cavity radii, the $2\gamma/r$ term has an effect of reducing the cavity growth rate, Equation 3. It is reasonable to assume that the $2\gamma/r$ term retards cavity growth negligibly when it is less than approximately 25% of the imposed stress level. Therefore, these maps can be used when

$$\sigma - (2\gamma - r) \gtrsim (3/4)\sigma \tag{18}$$

Rearranging the terms in Equation 18, the maps can be used to predict the transitions in cavity growth mechanisms when

$$r \gtrsim 8\gamma/\sigma \tag{19}$$

For a typical value of $\gamma = 1\,J\,m^{-2}$, the above requirement limits the use of these cavity growth maps to cavity radii greater than approximately 0.8 μm for a stress level of 10 MPa and 0.08 μm for a stress level of 100 MPa.

5. Comparison with experimental results

In this section, the predictions of the cavity growth maps will be compared with the experimental results on cavitation in three superplastic materials. The experimental results were chosen to demonstrate the use of the cavity growth maps when either grain boundary or lattice diffusion is important. It is relevant to note that diffusional growth processes generally lead to the development of rounded cavities whereas the power-law growth mechanism results in

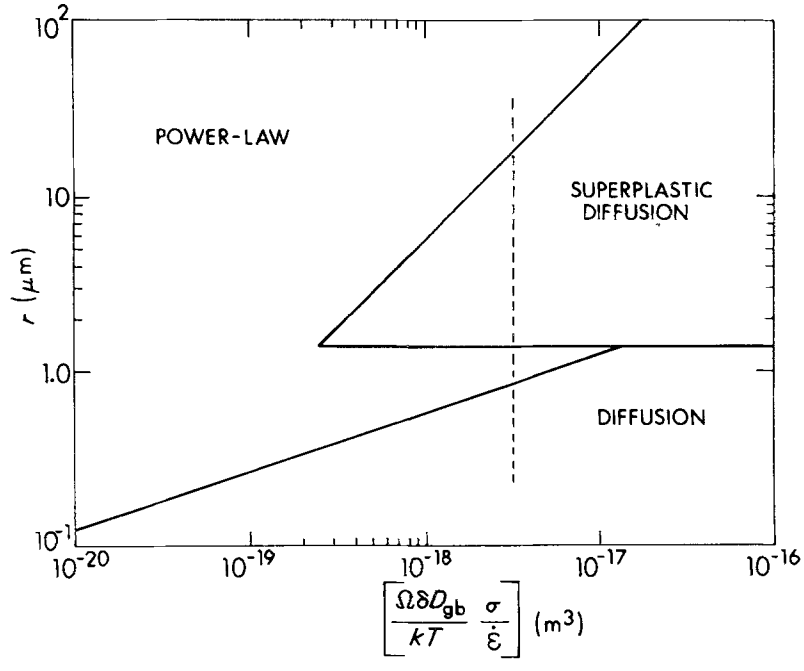

Figure 8 A cavity growth map of cavity radius against the parameter $\Omega\delta D_{gb}\sigma/kT\dot{\varepsilon}$ for a superplastic material with a grain size of 2.8 μm.

TABLE III Data used to calculate the cavity growth rates

Patermeter (units)		Cu–2.8% Al–1.8% Si–0.4% Co		Cu–38% Zn–15% Ni		Al–5.5% Zn–2.2% Mg–1.6% Cu	
		Value	Reference	Value	Reference	Value	Reference
γ	(Jm^{-2})	1.1	22	1.2	14	0.55	31
Ω	(m^3)	1.2×10^{-29}	8	1.1×10^{-29}	14	1.7×10^{-29}	32
D_{ogb}*	($m^2\,sec^{-1}$)	1×10^{-5}	8	1×10^{-5}	14	1×10^{-4}	8
Q_{gb}*	($kJ\,mol^{-1}$)	103	8	157.2	26, 27	84	8
D_l	($m^2\,sec^{-1}$)	–	–	–	–	$1.7 \times 10^{-4} \exp\left(-\frac{142000}{8.3T}\right)$	8
T	(K)	823	2	853	14	789	31
σ	(MPa)	12	2	25	14	5	31
$\dot{\varepsilon}$	(sec^{-1})	1.3×10^{-5}	2	5.5×10^{-4}	14	2×10^{-4}	31

*$D_{gb} = D_{ogb} \exp(-Q_{gb}/RT)$, where D_{ogb} is a frequency factor, Q_{gb} is the activation energy for grain boundary diffusion and R is the gas constant.

cavities that tend to be elongated along the tensile axis. The change in cavity morphology with cavity growth mechanism has been used successfully to rationalize the experimental results on cavity growth in several superplastic materials [2, 13, 23, 24].

5.1. Grain boundary diffusion dominates lattice diffusion

5.1.1. Cu–2.8% Al–1.8% Si–0.4% Co

This commercial copper-based superplastic alloy had a grain size of 2.8 μm; it was tested at a temperature of 823 K and a strain rate of $1.3 \times 10^{-5}\,sec^{-1}$ [2]. A microstructural examination of the specimen deformed to failure revealed that cavities with radii less than ~ 15–$20\,\mu m$ were rounded whereas those with radii greater than ~ 25–$30\,\mu m$ were elongated along the tensile axis [2, 20]. Fig. 8 is a map for cavity growth in a superplastic material with a grain size of 2.8 μm. Calculations indicate that for the experimental conditions used [2], the value of the parameter $\Omega\delta D_{gb}\sigma/kT\dot{\varepsilon} = 3.2 \times 10^{-18}\,m^3$; the data used for this evaluation are given in Table III. The experimental conditions are represented in Fig. 8 by a vertical broken line at $\Omega\delta D_{gb}\sigma/kT\dot{\varepsilon} = 3.2 \times 10^{-18}\,m^3$.

Fig. 8 predicts that cavities with radii $\lesssim 0.8\,\mu m$ will grow by the diffusional growth mechanisms whereas those with radii between ~ 0.8 and $1.4\,\mu m$ will grow by a power-law growth mechanism. However, in regions close to the line separating two growth mechanisms, both of the mechanisms will contribute significantly to cavity growth. Therefore, it is reasonable to assume from Fig. 8 that there is a direct transition from the diffusional to the superplastic diffusional growth mechanism at a cavity radius of $\sim 1\,\mu m$. Finally, at a cavity radius of $\sim 18\,\mu m$, there is a transition from the superplastic diffusional to the power-law growth mechanism. Thus, the cavity growth map shown in Fig. 8 predicts that cavities with radii $\lesssim 18\,\mu m$ will be rounded due to the dominance of diffusional growth processes whereas cavities with radii $\gtrsim 18\,\mu m$ will be elongated along the tensile axis due to the dominance of the power-law growth mechanism. This theoretical prediction is in good agreement with the experimental observation of such a transition in cavity morphology at cavity radii of ~ 20 to $25\,\mu m$ [2, 20].

5.1.2. Cu–38% Zn–15% Ni

Livesey and Ridley [14, 25, 26] have performed extensive studies of cavitation in this alloy. The material had a grain size of $\sim 3\,\mu m$ and the testing temperature was 853 K [14]. For the experimental conditions used, the value of the parameter $\Omega\delta D_{gb}\sigma/kT\dot{\varepsilon}$ is determined to be $4.8 \times 10^{-23}\,m^3$ (Table III). It is reasonable to interpret cavity growth in the Cu–38% Zn–15% Ni alloy using Fig. 8 that was drawn for a grain size of 2.8 μm. Inspection of Fig. 8 indicates that the superplastic diffusional growth mechanism is not relevant for values of the parameter $\Omega\delta D_{gb}\sigma/kT\dot{\varepsilon}$ less than

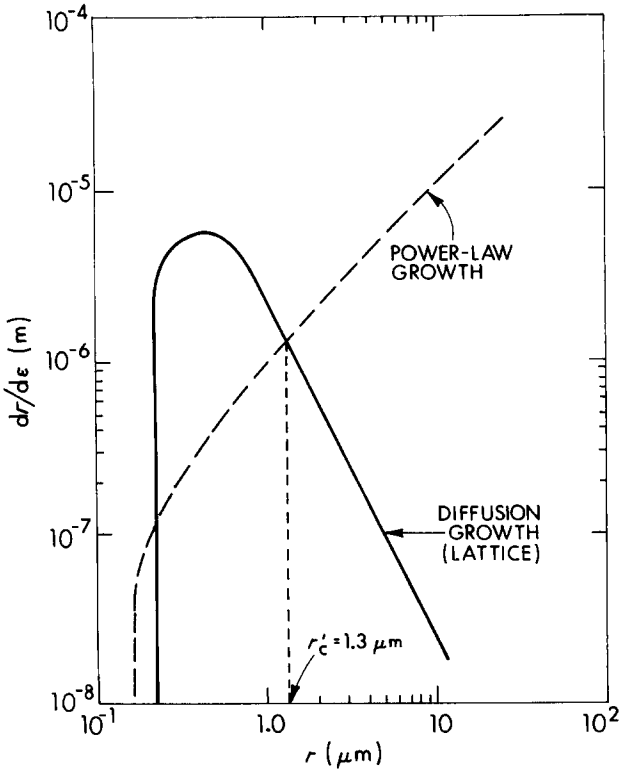

Figure 9 Cavity growth rate against the cavity radius for the Al–5.5% Zn–2.2% Mg–1.6% Cu alloy deformed at a strain rate of $2 \times 10^{-4}\,sec^{-1}$ and a temperature of 789 K.

$\sim 2 \times 10^{-19}$ m^3. In addition, for the experimental value of the parameter $\Omega\delta D_{gb}\sigma/kT\dot{\varepsilon} = 4.8 \times 10^{-23}$ m^3, the value of r_c is significantly less than 0.1 μm. It is therefore suggested that, upon nucleation, cavity growth in this material occurs solely by the power-law growth mechanism. This conclusion is in agreement with the detailed analysis of cavity growth in this alloy by Stowell [1, 28] and Livesey and Ridley [14, 26, 27].

5.2. Lattice diffusion dominates grain-boundary diffusion

5.2.1. Al–5.5% Zn–2.2% Mg–1.6% Cu

This alloy has considerable potential for commercial applications in the aerospace industry [29]. Extensive studies indicate that 789 K is the optimum temperature for the superplastic forming of the alloy [30]. The material typically has a grain size of ~ 15 μm and superplastic deformation usually leads to the occurrence of large elongated cavities [30–33]. In superplastic materials, the inter-cavity spacing is usually greater than the grain size and therefore it is assumed for the present analysis that $\lambda \simeq 2d = 30$ μm. Using the values of D_l and D_{gb} for pure aluminium (Table III) and Equation 6, the value of the parameter ψ is determined to be $\simeq 5$. This calculation indicates that, for the experimental conditions used in this alloy, diffusional cavity growth occurs predominantly by the lattice diffusion of vacancies since the value of ψ is significantly greater than 1.

Fig. 9 shows the variation in cavity growth rate against cavity radius on a logarithmic scale. The data used to plot Fig. 9 are summarized in Table III. An examination of Fig. 9 suggests that cavities with radii $\gtrsim 1.3$ μm will grow by the power-law growth mechanism. For the experimental conditions corresponding to $\sigma/\dot{\varepsilon} = 2.5 \times 10^4$ MPa sec^{-1} and $T = 789$ K, calculations indicate that the parameter $\Omega\lambda D_l\sigma/\pi kT\dot{\varepsilon} = 2.4 \times 10^{-17}$ m^3. As noted earlier, Fig. 5 can be used as a cavity growth map for all superplastic materials when lattice diffusion dominates over the grain boundary diffusion of vacancies. An analysis of cavity growth based on Fig. 5 predicts that, when a vertical line is erected at $\Omega\lambda D_l\sigma/\pi kT\dot{\varepsilon} = 2.4 \times 10^{-17}$ m^3, the transition from the lattice diffusional to the power-law cavity growth mechanism occurs at a cavity radius of ~ 1.3 μm. The above analysis indicates that cavities with radii $\gtrsim 1.3$ μm will be elongated along the tensile axis due to the dominance of the power-law growth mechanism. This theoretical prediction is in agreement with the experimental observation of large elongated cavities in this alloy [30–33] and a detailed analysis of cavity growth by Bampton and Raj [32].

6. Summary and conclusions

1. Appropriate cavity growth mechanisms for superplastic materials are considered in detail and the contribution of lattice diffusion to cavity growth is included in the overall analysis of cavity growth.

2. Two different types of cavity growth maps are developed to depict the variation in dominant cavity growth mechanisms. First, cavity growth maps of cavity radius, r, against the parameter $\Omega\delta D_{gb}\sigma/kT\dot{\varepsilon}$ are constructed for a fixed grain size. Second, cavity growth maps of r against the grain size, d, are developed for a fixed value of the parameter $\Omega\delta D_{gb}\sigma/kT\dot{\varepsilon}$.

3. Simple procedures are outlined for the construction of the two types of maps for materials with different grain sizes and for materials tested with different values of the parameter $\Omega\delta D_{gb}\sigma/kT\dot{\varepsilon}$.

4. Conditions are developed to predict the appropriate transitions in cavity growth mechanisms with increasing radii and the limitations of these maps at very small cavity radii are discussed.

5. It is demonstrated that the predictions of the cavity growth maps are in agreement with the experimental results on cavitation in several superplastic materials.

Acknowledgement

The author would like to acknowledge a useful discussion with Professor Terence G. Langdon at the University of Southern California.

References

1. M. J. STOWELL, in "Superplastic Forming of Structural Alloys", edited by N. E. Paton and C. H. Hamilton (The Metallurgical Society of AIME, Warrendale, Pa., U.S.A., 1982) p. 321.
2. A. H. CHOKSHI, PhD thesis, University of Southern California, Los Angeles (1984).
3. R. D. SCHELLENG and G. H. REYNOLDS, *Metall. Trans.* **4** (1973) 2199.
4. C. C. BAMPTON and J. W. EDINGTON, *J. Eng. Mater. Technol.* **105** (1983) 55.
5. M. F. ASHBY, *Acta Metall.* **20** (1972) 887.
6. F. A. MOHAMED and T. G. LANGDON, *Metall. Trans.* **5** (1974) 2339.
7. T. G. LANGDON and F. A. MOHAMED, *J. Mater. Sci.* **13** (1978) 1282.
8. H. J. FROST and M. F. ASHBY, in "Deformation Mechanism Maps" (Pergamon Press, Oxford, 1982).
9. M. F. ASHBY, C. GANDHI and D. M. R. TAPLIN, *Acta Metall.* **27** (1979) 699.
10. L-E. SVENNSON and G. L. DUNLOP, *Int. Met. Rev.* **26** (1981) 109.
11. *Idem*, in "Creep in Structures", edited by A. R. S. Ponter and D. R. Hayhurst (Springer-Verlag, Berlin, 1981) p. 445.
12. D. A. MILLER and T. G. LANGDON, *Scripta Metall.* **14** (1980) 179.
13. *Idem, Metall. Trans. A* **10A** (1979) 1869.
14. D. W. LIVESEY and N. RIDLEY, *ibid.* **13A** (1982) 1619.
15. D. HULL and D. E. RIMMER, *Phil. Mag.* **4** (1959) 673.
16. W. BEERE and M. V. SPEIGHT, *Met. Sci.* **12** (1978) 172.
17. F. DOBES and J. CADEK, *Scripta Metall.* **4** (1970) 1005.
18. J. W. HANCOCK, *Met. Sci.* **10** (1976) 319.
19. F. A. McCLINTOCK, *J. Appl. Mech.* **35** (1968) 363.
20. A. H. CHOKSHI and T. G. LANGDON, in "Superplasticity", edited by B. Baudelet and M. Cuery (CNRS, Paris, 1985) p. 21.
21. B. BURTON, *Phil. Mag.* **30** (1974) 953.
22. R. RAJ and M. F. ASHBY, *Acta Metall.* **23** (1975) 653.
23. D. A. MILLER and T. G. LANGDON, *Trans. Jpn Inst. Met.* **21** (1980) 123.
24. A. H. CHOKSHI, *J. Mater. Sci. Lett.* in press.
25. D. W. LIVESEY and N. RIDLEY, *Metall. Trans.* **9A** (1978) 519.
26. N. RIDLEY, D. W. LIVESEY and A. K. MUKHERJEE, *J. Mater. Sci.* **19** (1984) 1321.
27. D. W. LIVESEY, N. RIDLEY and A. K. MUKHERJEE, *ibid.* **19** (1984) 3602.
28. M. J. STOWELL, *Met. Sci.* **14** (1980) 267.

29. C. H. HAMILTON, C. C. BAMPTON and N. E. PATON, in "Superplastic Forming of Structural Alloys", edited by N. E. Paton and C. H. Hamilton (The Metallurgical Society of AIME, Warrendale, Pa., USA, 1982) p. 173.
30. C. C. BAMPTON and J. W. EDINGTON, *Metall. Trans.* **13A** (1982) 1721.
31. A. K. GHOSH, in "Deformation of Polycrystals: Mechanisms and Microstructures", edited by N. Hansen, A. Horsewell, T. Leffers and H. Lilholt (Risø National Laboratory, Røskilde, Denmark, 1981) p. 277.
32. C. C. BAMPTON and R. RAJ, *Acta Metall.* **30** (1982) 2043.
33. C. C. BAMPTON, M. W. MAHONEY, C. H. HAMILTON, A. K. GHOSH and R. RAJ, *Metall. Trans.* **14A** (1983) 1583.

Received 11 April
and accepted 14 August 1985